Energy Proceedings
Vol 49, 2024
ISSN 2004-2965

Enhancing Metal Hydride – Phase Change Material Hydrogen Storage Systems Efficiency with Expanded Graphite#

Marco Maggini[1], Giacomo Falcucci[2], Andrea L. Facci[1*], Stefano Ubertini[1]

1 Department of Economics, Engineering, Society and Business Administration, University of Tuscia, 01100 Viterbo, Italy

2 Department of Enterprise Engineering "Mario Lucertini", University of Rome "Tor Vergata", Via del Politecnico 1, 00133 Rome, Italy; John A. Paulson School of Engineering and Applied Physics, Harvard University, 33 Oxford Street, 02138 Cambridge, Massachusetts, USA.

(Corresponding Author: andrea.facci@unitus.it)

ABSTRACT

Hydrogen storage systems and, specifically, metal hydride-based systems, hold a significant potential when it comes to finding safe, affordable, and efficient energy storage solutions [1-3]. A challenge often associated with most metal hydride compounds is building an efficient Heat Management System to prevent the hydride temperature to diverge from equilibrium and, thus, slow down the storage process [4]. We analyze a hybrid Metal Hydride – Phase Change Material (MH-PCM) configuration, where the PCM surrounds the MH powder and works as Thermal Storage Unit (TSU). During desorption of hydrogen (endothermic), the PCM provides heat to the MH by using the same energy that it had previously stored during the absorption stage (exothermic) [5]. However, PCMs suffer from low thermal conductivities, thus several Thermal Augmentation Systems (TAS) might be employed to try and solve this issue. Among them, we focus our attention on the addition of Expanded Natural Graphite (ENG) into the PCM. ENG has a high thermal conductivity and can be easily mixed within the PCM to form a composite. The reduction in gravimetric and volumetric density is a negative side effect of using ENG.

In this work, we numerically assess the impact of ENG by comparing the absorption and desorption processes of a baseline MH-PCM design and other layouts with increasing amounts of ENG.

The results show that the overall cycle time is reduced by 20.9% when increasing the ENG volume fraction from 0% to 25%. The gravimetric density drops by 12.3%, thus suggesting the increase in the storage system weight and size. The average inlet and outlet power increase from 2.7 kW to 3.6 kW and from 1.2 kW to 1.45 kW, respectively.

Keywords: renewable energy resources, hydrogen storage, metal hydride, phase change material, energy systems, climate change

NOMENCLATURE

Abbreviations	
MH	Metal Hydride
PCM	Phase Change Material
RES	Renewable Energy Source
Symbols	
$\mathcal{L}$	Length
D	Diameter
m	Mass
M	Molecular weight
S_C	Stoichiometric coefficient
f	Hydrogen mass flow rate
r	Reaction rate
C	Kinetic constant
E	Activation energy
ΔH	Reaction enthalpy
ΔS	Reaction entropy
β	Reaction plateau slope coefficient
Subscripts	
a	Absorption
d	Desorption

1. INTRODUCTION

Hydrogen holds a significant potential when it comes to finding new and innovative energy storage solutions, as it can either be stored in gaseous, liquid, or solid form and boast flexibility as for integration with Renewable Energy Sources (RES) [6]. The first two methods pertain to the physical-based storage methods, where the density of hydrogen is increased by increasing the pressure or lowering the temperature, respectively. Solid-state hydrogen storage relies on the different concept of either trapping hydrogen by adsorption (so-called physisorption) or making it react with a metal or metal alloys (so-called chemisorption). In particular, the

This is a paper for the 16th International Conference on Applied Energy (ICAE2024), Sep. 1-5, 2024, Niigata, Japan.

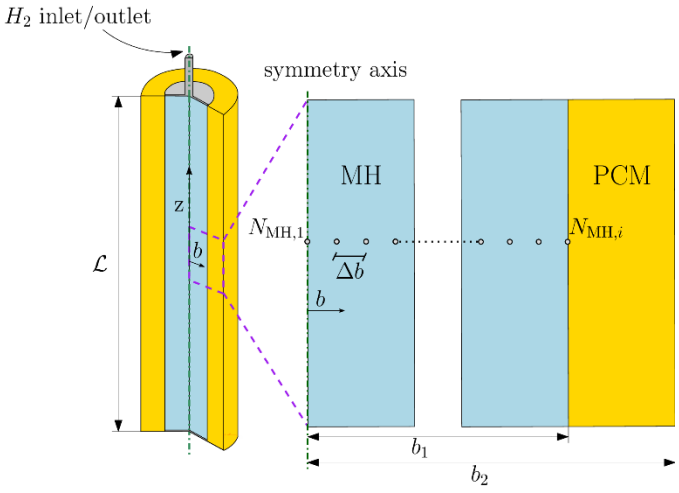

Fig. 1. Schematic of MH-PCM storage system.

latter option holds relevant promises of reducing storage pressure and temperature, while increasing the storage efficiency [7]. The reversible reaction between hydrogen and metal compounds to form Metal Hydrides is one of the solid-state storage options.

The most relevant issue of employing MHs to store hydrogen is the Thermal Management System. In fact, the hydrogenation is an exothermic reaction, whereas the dehydrogenation is an endothermic reaction. Thus, in order for the charge and discharge processes to be fast, the MH temperature must be controlled, i.e., reduced during charge and increased during discharge [4].

In these regards, much research is now focused on finding efficient and lightweight systems to dispose of the charge heat and provide the discharge heat. The most effective way is by employing active systems, i.e., heat exchangers and heat pipes. This comes with the issue of using an external energy supply. Among the passive systems, two are significantly noteworthy: (i) increasing the materials' thermal diffusivity (e.g., by including carbon nano-particles or expanded graphite) and (ii) coupling the MH with a Phase Change Material (PCM). The latter option provides a passive way to exchange heat between the MH and the external environment, where the PCM absorbs the hydrogenation heat while melting, and releases the same heat towards the MH during dehydrogenation while solidifying [8].

In this work, we explore both solution by investigating the behavior of a hybrid MH-PCM hydrogen storage system as a function of the volume fraction of Expanded Graphite dispersed in the PCM. To the best of our knowledge, no previous works focused on the impact of ENG in a hybrid MH-PCM, whereas only plain MH- or mixed MH-Heat Exchangers option have been investigated with ENG.

The paper is organized as follows: in Section 2 we outline the numerical methodology employed, together with the relevant assumptions, the numerical solutions, and the model validation. In Section 3 we present and discuss our findings and main results, with the aim to highlight the significance in terms of providing guidelines for the design of such hybrid hydrogen storage systems. In Section 4, we draw the conclusions.

2. METHODOLOGY

2.1 System description

The system is made of an inner cylinder of MH ($LaNi_5$), with porosity $\xi = 0.5$, length $\mathcal{L} = 1.27$ m, and diameter $D = 2.54$ cm (see Fig. 1). Such a configuration has been retrieved by previous research of the authors [9] which describes it as the recommended layout to store 1 kWh of energy. Such inner cylinder can therefore contain 2.34 kg of $LaNi_5$. If a gravimetric density $w = \frac{m_{H_2}}{m_{MH}} = \frac{S_C \cdot M_{H_2}}{M_{MH}} = 1.38\%$ is accounted for, it can then store 30.2 g of hydrogen.

The MH cylinder is surrounded by an external jacket of PCM ($LiNO_3 - 3H_2O$), with external radius b_2, which varies from case to case depending on the volume fraction of EG ε in the PCM. In fact, the higher ε, the lower the PCM latent heat of fusion. Therefore, a larger amount of PCM has to be used to store the same amount of thermal energy, thus the higher value of b_2.

During charge, hydrogen is supplied at the inlet pressure $p^a_{H_2} = 20$ bar, greater than the equilibrium pressure p_{eq}. During discharge, the outlet hydrogen pressure is $p^d_{H_2} = 1$ bar.

2.2 MH modeling

We make use of the following hypotheses to build out mathematical model: (i) gases are ideal and compressible; (ii) the porous medium is homogeneous; (iii) the thermos-physical properties of both MH and PCM are not a function of temperature; (iv) the pressure inside the vessel is homogeneous in space and constant in time ($p = p_{H_2}$); (v) MH and the hydrogen gas are in local thermal equilibrium; (vi) the natural convection within the PCM is neglected.

We base our mathematical conceptualization on the mass and energy conservation inside the MH domain, as follows [10]:

$$\frac{dm_{H_2}}{dt} = f_{H_2} - r \cdot m_{MH} \cdot w,$$

$$\frac{\partial T}{\partial t} = \alpha^e_{MH} \nabla^2 T + \dot{q}.$$

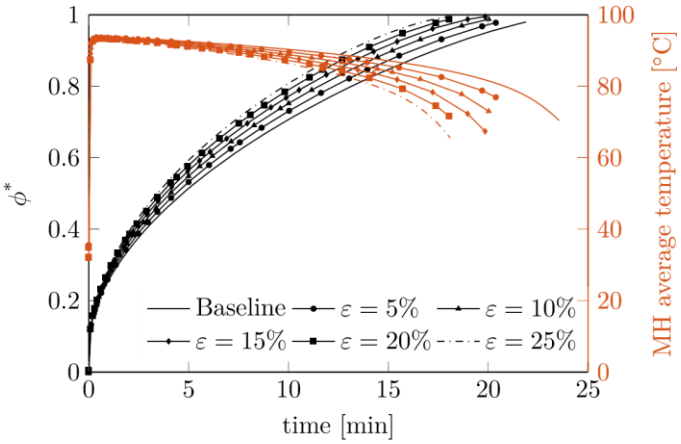

Fig. 2. Saturation level and MH average temperature for different ε in absorption.

Where $\alpha^e_{MH} = \frac{k^e}{(\rho c_p)^e}$ is the MH effective thermal diffusivity, and $\dot{q}$ is the volumetric heat source. In turn, k^e, $(\rho c_p)^e$ are calculated as described in [11]. In absorption and desorption, the reaction rate r is evaluated as follows:

$$r_a = C_a e^{-\frac{E_a}{RT}} \cdot \ln\frac{p_{H_2}}{p_{eq}} \cdot (1-\phi),$$

$$r_d = C_d e^{-\frac{E_d}{RT}} \cdot \frac{p_{H_2} - P_{eq}}{p_{eq}} \cdot \phi.$$

The state of charge (or saturation level) $\phi = \frac{m_{H_2}}{m_{MH}}$ is always between 0 and 1 and assess the evolution of the hydrogenation and dehydrogenation process. Finally, the equilibrium pressure is calculated as follows:

$$p_{eq} = p_0 e^{\frac{\Delta H}{RT} - \frac{\Delta S}{R} + \beta\left(\phi - \frac{1}{2}\right)}.$$

2.3 PCM modeling

We model the melting and solidification of the PCM through the enthalpy method, namely:

$$\rho_{PCM}\frac{\partial H}{\partial t} = k_{PCM}\nabla^2 T,$$

Where $H = c_{p_{PCM}} T$ is the enthalpy in the PCM. To investigate the impact of EG into the PCM, we modify the mathematical model with the Maxwell's mixing formulas [12]:

$$k^e_{PCM} = \frac{k_{PCM} \cdot (2k_{PCM} + k_{NP} - 2\varepsilon \cdot (k_{NP} - k_{PCM})}{2k_{PCM} + k_{NP} - \varepsilon \cdot (k_{NP} - k_{PCM})},$$

$$\rho^e_{PCM} = (1-\varepsilon) \cdot \rho_{PCM} + \varepsilon\rho_{NP},$$

$$c^e_{p_{PCM}} = \frac{1}{\rho^e_{PCM}} \cdot (1-\varepsilon) \cdot c_{p_{PCM}}\rho_{PCM} + \varepsilon c_{p_{NP}}\rho_{NP}.$$

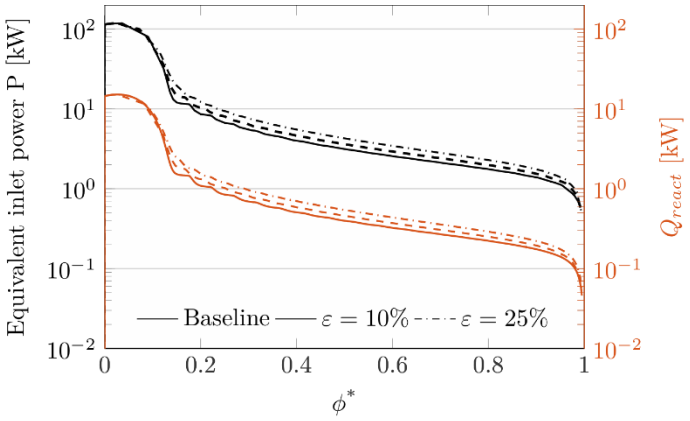

Fig. 3. Equivalent inlet power and volumetric heat developed for different ε in absorption.

The EG thermal conductivity k_{NP} is, in turn, a function of the carbon porosity, which we assume to be 65% [13]. Thus, $k_{NP} = 47$ W/mK. Finally, we calculate the amount of PCM, and thus, the total volume of the system as follows:

$$V_{PCM} = m_{H_2} \cdot \frac{\frac{\Delta H}{M_{H2}}}{\lambda_{PCM}\rho_{PCM}}.$$

Such volume is then a function of the PCM latent of fusion, which linearly varies with ε: $\lambda^e_{PCM} = \lambda_{PCM} \cdot (1-\varepsilon)$. Consequently, the value of the radius b_2 varies with ε, specifically increasing with it.

We vary the volume fraction of ENG in the PCM ε between 0% and 25%, which is typically considered a threshold for the validity of Maxwell's mixing formulations [14].

2.4 Numerical solution

According to the complete axi-symmetry of the investigated model, we only discretize the MH and the PCM domain along the radial direction, between $b = 0$ and $b = b_2$. The number of nodes in the MH is equal to 25, with a corresponding node-to-node distance of approximately 0.5 mm. The PCM is discretized maintaining the same node-to-node resolution of 0.5 mm, therefore the number of nodes varies depending upon the value of ε. We use a second order finite difference scheme for the spatial discretization while the numerical solution of the differential and algebraic equations is implemented in Matlab R2023b.

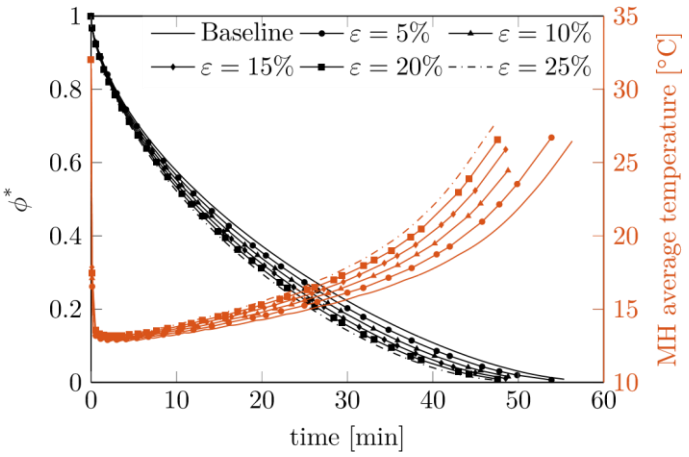

Fig. 4. Saturation level and MH average temperature for different ε in desorption.

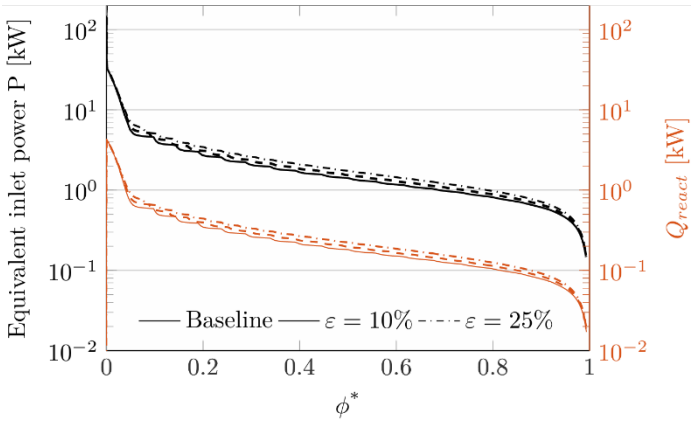

Fig. 5. Equivalent outlet power and volumetric heat developed for different ε in desorption.

3. RESULTS AND DISCUSSION

Fig. 2 shows the hydrogen storage state of charge ϕ^* as a function of time for different values of ENG volume fraction in the PCM. The correspondent temperature profiles are also shown. $\phi^* = \phi$ in absorption and $1 - \phi^*$ in desorption. The absorption reaction is 24.2% faster to reach 95% of saturation as the volume fraction of ENG increases from 0% to 25%. This is ascribable to the more efficient heat transfer between the MH and PCM, which allows for a better disposal of the hydrogenation heat. Therefore, more hydrogen reacts per unit time [15]. The average temperature inside the MH is, in fact, lower at higher ε. The faster cooling rate is clear for $t > 10$ min.

Fig. 3 shows the inlet equivalent power $P = f_{H_2} \cdot H_i$, where $H_i = 120 \times 10^3$ kJ is the lower heating value of hydrogen. P is therefore directly related to the amount of hydrogen flowing in the canister per unit time and aim of the present work is to increase such value. P increases with ε only for $\phi^* > 15\%$, whereas the early stage is dominated by the reaction kinetics and not by the heat exchange efficiency. In other words, for $\phi^* < \approx 0.15$, the absorption into the MH is not a function of the heat disposal rate, and improving the PCM's thermophysical properties does not have any relevant impact on the reaction. At $\phi^* \approx 0.15$, a shift in trend is evident, where P drastically reduces and acquires a nearly linear behavior with ε. Conversely, for $\phi^* > 0.15$, the reaction is mainly dominated by the heat disposal rate and improves if the PCM's thermal diffusivity is increases with EG inclusions. Fig. 3 also shows the heat developed during the absorption phase $Q_{react}^{abs} = \Delta H \cdot r \cdot \frac{\rho_{MH} \cdot \xi}{M_{H_2}}$ as a function of ϕ^* and for different EG volume fractions. If more heat is developed during the reaction, this is a clear proxy of a greater reaction rate. Correspondingly with P, also the amount of heat developed during the reaction increases with EG amount, indicating a faster absorption reaction.

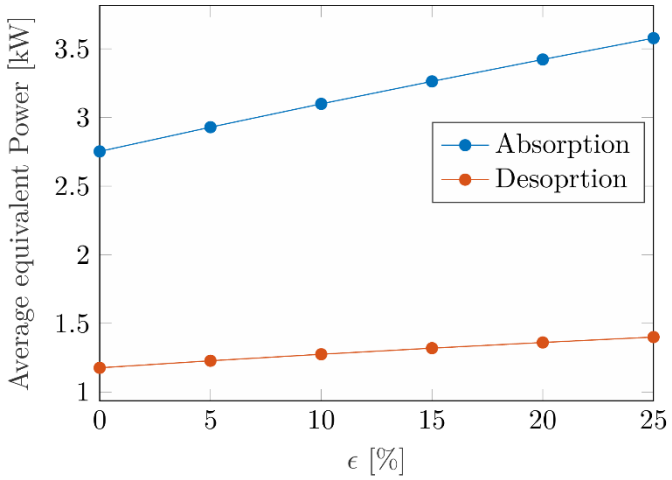

Fig. 6. Average absorption and desorption power as function of ε.

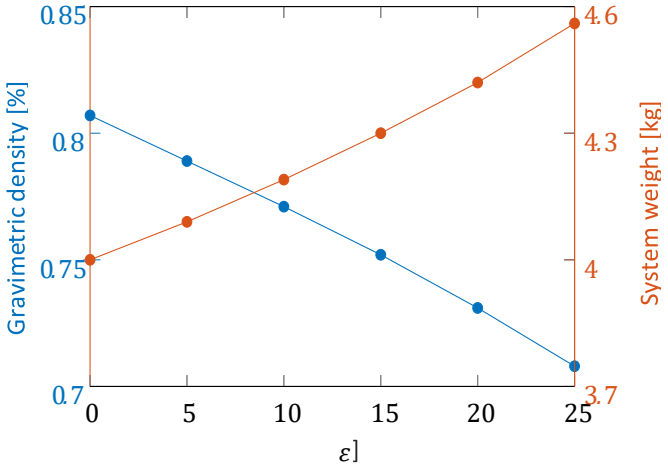

Fig. 7. Gravimetric density and system weight as function of ε.

In desorption, the reaction is 17.5% faster to release 95% of hydrogen when increasing ε from 0% to 25% (see Fig. 4). Correspondingly, the average temperature inside the MH is comparatively higher when ε is higher. This is due to the better heat transfer inside the PCM and, thus, the better heat exchange between the MH and PCM, which allows for a faster provision of heat from the latter. This quickens the dehydrogenation reaction. The equivalent outlet power P increases with ε, suggesting the increase in hydrogen mass flow rate (see Fig. 5). The reaction heat Q_{ract}^{des} also increases, indicating a greater reaction rate inside the MH.

In Fig. 6, the average values of the absorption and desorption power are shown as function of ε. We comment that the absorption power is consistently higher than the desorption power, indicating that the latter phase is the critical one when addressing the power augmentation strategies. It is also evident that the slope of the $P_{avg}^{abs}\ vs.\ \varepsilon$ curve is greater than that of $P_{avg}^{des}\ vs.\ \varepsilon$. This indicates that adding ENG to the PCM is more effective for the charge phase than for the discharge phase. Finally, we remind that including ENG in the PCM comes with a disadvantage, which is the reduction in energy density of the storage system. In fact, by adding ENG in the PCM, the capacity of the latter to transfer heat with the MH is impaired, inasmuch a fraction of the original volume is now occupied by the carbon inclusions. Therefore, in order for the PCM mass to be constant as ε increases, the external radius b_2 has to increase as well. This effect can be appreciated in Fig. 7, where the gravimetric density (hydrogen stored per unit mass) and the total system weight are plotted as a function of ε. The energy density per unit mass decreases of approximately -12.3%, while the total mass (MH + PCM) increases from 4 kg to 4.6 kg, as a results of the increased total volume of PCM employed to satisfy the same heat demand.

4. CONCLUSIONS

A hybrid Metal Hydride-Phase Change Material hydrogen storage system was investigated with a 1D numerical simulation in terms of charge/discharge time and equivalent power. Several configurations were analyzed, where Expanded Graphite was inserted in the PCM at different volume fractions.

Results show that increasing the ENG volume fraction from 0% to 25% increases the equivalent inlet and outlet powers of 30% and 19%, respectively. Also, the latent heat of fusion is linearly decreasing with the EG volume fraction, thus increasing the total volume occupied by the system. In turn, this decreases the mass energy density of the storage system from 0.807% to 0.708% (-12.3%) in the same range of EG volume fraction.

Therefore, a trade-off must be accounted for every time ENG is included in the PCM. For stationary applications, the energy density is not of primary importance. We also conclude that adding ENG in the PCM in a MH-PCM hydrogen storage system is mainly effective for reducing the charge time, instead of the discharge time.

ACKNOWLEDGEMENT

Roma technopole and Partenariati estesi PE2.

This work has been prepared as a partial fulfilment of the "European Specialization School in Sustainable Energy" and supported by the Horizon Europe Project No 101075587, call HORIZON-CL5-2021-D3-02 "SKILL TO BOOST INNOVATION AND PROFESSIONAL FULFILLMENT IN A SUSTAINABLE ECONOMY".

REFERENCE

[1] A. Rosen and S. Koohi-Fayegh, Energy, Ecology and Environment, 1 (2016) 10 – 29.

[2] J. O. Abe et al., International Journal of Hydrogen Energy, 44 (2019) 5072 – 15086.

[3] S. D. Patil et al., International Journal of Hydrogen Energy, 38 (2013) 942–951.

[4] A. L. Facci et al., Energies, 14 (2021) 1554.

[5] H. Nazir et al., International Journal of Heat and Mass Transfer, 129 (2019) 491 – 523.

[6] F. Zhang, P. Zhao, M. Niu, J. Maddy, International journal of hydrogen energy, 41 (2016) 14535–14552.

[7] C. Drawer, J. Lange, M. Kaltschmitt, Journal of Energy Storage, 77 (2024).

[8] B. M. Diaconu, M. Cruceru, L. Anghelescu, Journal of Energy Storage, 61 (2023).

[9] M. Maggini, G. Falcucci, A. Rosati, S. Ubertini, A. L. Facci, Journal of Energy Storage, 93 (2024) 112230.

[10] B. Talaganis, G. Meyer, P. Aguirre, International journal of hydrogen energy, 36 (2011) 13621–1363.

[11] Y. Ye, J. Lu, J. Ding, W. Wang and J. Yan, Applied Energy, 278 (2020) 115682.

[12] G. Di Ilio et al., Journal of Scientific Computing, 83 (2020)

[13] H.-P. Klein and M. Groll, Int. J. of Hydrogen Energy, 29 (2004), 1503 – 1511

[14] K. Pietrak and T. S. Wiśniewski, J. of Power Technologies, 95(2015) 14 – 24

[15] Krastev V., Bella G., Falcucci G., Bartolucci L., Cordiner S. and Mulone V., ECOS 2023 (2023), 2183 – 2193